Developmental Biology 448 (2019) 199–209

Contents lists available at ScienceDirect

Developmental Biology

journal homepage: www.elsevier.com/locate/developmentalbiology

Original research article

Initial characterization of Wnt-Tcf functions during *Ciona* heart development

Nicole A. Kaplan, Wei Wang, Lionel Christiaen*

Center for Developmental Genetics, Department of Biology, New York University, New York, NY, USA

A B S T R A C T

In vertebrate embryos, the cardiopharyngeal mesoderm gives rise to both cardiac and branchiomeric head muscles. The canonical Wnt signaling pathway regulates many aspects of cardiomyocyte specification, and modulates a balance between skeletal and cardiac myogenesis during vertebrate head muscle development. However, the role of Wnt signaling during ascidian cardiopharyngeal development remains elusive. Here, we documented the expression of Wnt pathway components during cardiopharyngeal development in *Ciona*, and generated tools to investigate potential roles for Wnt signaling, and its transcriptional effector Tcf, on heart vs. pharyngeal muscle fate specification. Neither focused functional analyses nor lineage-specific transcriptome profiling uncovered a significant role for *Tcf* during early cardiac vs. pharyngeal muscle fate choice. By contrast, Wnt gene expression patterns of *Frizzled4* and *Lrp4/8* and CRISPR/Cas9-mediated *Tcf* knock-down suggested a later requirement for Wnt signaling during heart morphogenesis and/or cardiomyocyte differentiation. This study provides a provisional set of reagents to study Wnt signaling function in *Ciona*, and promising insights for future analyses of Wnt functions during heart organogenesis.

1. Introduction

The early molecular events underlying cardiogenesis are highly conserved across metazoans (Davidson and Erwin, 2006; Olson, 2006). Despite differences in adult heart morphology, a core set of cardiac transcription factors is conserved from insects to vertebrates and defines the heart-forming field during embryogenesis. These core factors include homologs of the homeodomain-containing transcription factor *Nk4/Nkx2–5*, *HAND*-family basic helix-loop-helix (bHLH) transcription factors, and zinc finger transcription factors of the *GATA* family (reviewed in Bodmer and Venkatesh (1998)). How heart progenitors emerge from multipotent mesodermal progenitors is a long-standing question in basic developmental biology and biomedical cardiovascular research.

In addition to a conserved set of cardiac molecular determinants, the developmental relationship between heart and head musculature has deep evolutionary origins. The vertebrate heart forms from two sources of mesodermal progenitors, named the first and the second heart fields (Buckingham et al., 2005; Meilhac et al., 2004). The second heart field derivatives originate from pharyngeal mesoderm which gives rise to both cardiomyocytes and branchiomeric muscles (Lescroart et al., 2015, 2014, 2012, 2010; Tirosh-Finkel et al., 2006; Tzahor and Evans, 2011). The latter form the musculature of the vertebrate jaw and parts of the face. Regulatory genes in the pharyngeal mesoderm are highly conserved among chordates, such as *Nk4/Nkx2-5* (Prall et al., 2007), the LIM/homeobox transcription factor *Islet1* (Harel et al., 2009; Nathan et al., 2008), and the T-Box transcription factor *Tbx1/10* (Chen et al., 2009; Liao et al., 2008).

The influence of extracellular signaling pathways on the developing heart is also fundamental. Among them is the canonical Wnt/β-catenin pathway, which influences cardiogenesis in a variety of contexts and organisms (Naito et al., 2006; Tzahor, 2007; Ueno et al., 2007). In Drosophila, *wingless* (the *Wnt-1* homolog) is necessary for heart formation and is sufficient to expand the cardiac mesoderm, leading to an excess of *tinman*-positive (*Nkx2-5* homolog) cardiac precursors (Park et al., 1996; Wu et al., 1995). Additionally, mesoderm-specific expression of a dominant-negative form of *pangolin/dTCF*, which lacks the N-terminal β-catenin binding domain, abolishes heart progenitor formation (Park et al., 1998). During vertebrate heart development, Wnt signaling regulates many aspects of cardiomyocyte specification and differentiation in a stage-specific manner, as there are distinct temporal requirements for either Wnt signaling activity or inhibition (reviewed in (Gessert and Kühl (2010) and Tzahor (2007)). Wnt activity is required early to specify cardiogenic mesoderm, but then needs to be inhibited in order to form cardiomyocytes from this tissue. After specification, Wnt/β-catenin signaling is required for the proliferation of cardiac

* Corresponding author.
E-mail address: lc121@nyu.edu (L. Christiaen).

https://doi.org/10.1016/j.ydbio.2018.12.018
Received 28 June 2018; Received in revised form 14 December 2018; Accepted 17 December 2018
Available online 08 January 2019
0012-1606/

progenitors, particularly in the second heart field, where it directly regulates *Isl1* expression (Lin et al., 2007). Finally, Wnt has an inhibitory effect on the terminal differentiation of cardiomyocytes (reviewed in Cohen et al. (2008) and Gessert and Kühl (2010)).

The regulation of Wnt activity is not only critical in the developing heart; it is also important during vertebrate head muscle development. Studies in chick embryos demonstrated that antagonizing canonical Wnt and Bmp signals promotes skeletal myogenesis in the head (Tzahor et al., 2003). In explants, BMP antagonists activate skeletal muscle differentiation markers, while the Wnt antagonist Frzb instead induces the expression of cardiac markers (Tzahor et al., 2003). Prior to gastrulation in zebrafish embryos, canonical Wnt activity promotes cardiac specification (Ueno et al., 2007), while on the contrary, it is necessary and sufficient to inhibit pharyngeal muscle development (Mandal et al., 2017). Excess Wnt signaling during this developmental time promotes the expansion of first heart field progenitors at the expense of second heart field and pharyngeal muscle progenitor domains (Mandal et al., 2017). Hence, Wnt signaling activation vs. inhibition may be involved in modulating a balance between skeletal and cardiac myogenesis during vertebrate development. While the effects of Wnt signaling have been examined in the context of heart and head muscle development in vertebrates, they have not yet been explored in ascidians, which possess multipotent cardiopharyngeal precursors during development and highly conserved regulatory activities underlying lineage-specific cell identities.

Ciona is a member of the Tunicates, which are the closest relatives of the vertebrates (Delsuc et al., 2006; Putnam et al., 2008). The *Ciona* larva possesses a notochord and a dorsal neural tube, among other chordate-specific features (Satoh, 1994). In the 110-cell gastrula, a single blastomere on each side of the bilaterally symmetric embryo, called the B7.5 cell based on Conklin's nomenclature, expresses the bHLH transcription factor *Mesp* (Davidson and Levine, 2003; Satou et al., 2004). *Mesp* expression specifies the heart field in both *Ciona* and vertebrate embryos (Davidson and Levine, 2003; Saga et al., 1999; Satou et al., 2004). Similar to vertebrate embryos, cardiac mesoderm induction requires β-catenin inputs. In *Ciona*, *Mesp* activation is restricted to the B7.5 blastomeres by the overlapping expression domains of zygotic Tbx6 and Lhx3, which are activated by maternal Macho-1 and β-catenin, respectively (Christiaen et al., 2009). Following *Mesp* induction, the B7.5 cells move anteriorly and undergo a symmetric division followed by an asymmetric division, forming two larger anterior tail muscle cells (ATMs) that remain in the tail, and two smaller multipotent cardiopharyngeal progenitors, called trunk ventral cells (TVCs; Fig. 1A). TVCs are asymmetrically induced by localized activation of an FGF-MAPK/Ets signaling cascade (Davidson et al., 2006), and migrate as a polarized pair away from the ATMs, further into the ventral trunk of the embryo. Downstream of this cascade, TVC genes are activated *de novo*, such as the forkhead transcription factor *Foxf* (Beh et al., 2007) and the HAND-like gene *Hand-related* (*Hand-r*/*NoTrlc*) (Satou et al., 2004), or maintained specifically in the TVCs (e.g. *Ets1/2*).

Following migration, TVCs on each side of the embryo meet at the ventral midline and divide in a stereotyped medio-lateral orientation at approximately 13.5 h post fertilization (hpf), forming smaller first heart precursors (FHPs) medially and larger secondary TVCs (STVCs) laterally (Fig. 1A; Stolfi et al., 2010). Immediately after this asymmetric division, STVCs activate the *de novo* transcription of the conserved pharyngeal mesoderm marker *Tbx1/10* (Wang et al., 2013). At approximately 15.5 hpf, STVCs divide in an asymmetric and oriented fashion giving rise to second heart precursors (SHPs) medially and pharyngeal muscle precursors laterally, known as atrial siphon muscle precursors (ASMPs). Downstream of *Hand-r* and *Tbx1/10*, the DNA-binding transcription factor *Ebf* (aka *Collier/OLF/Ebf*) is activated exclusively in ASMFs and specifies ASM fate (Razy-Krajka et al., 2014; Stolfi et al., 2010). TVCs are transcriptionally primed for both ASM and heart specification, as they express genes that will restrict to either the FHPs, or to the STVCs and then ASMFs, with subsequent divisions (Razy-Krajka et al., 2014). Throughout this progressive restriction, the segregation of heart and ASM programs is enforced by cross-antagonisms whereby *Tbx1/10* inhibits *Gata4/5/6* and the cardiac program in the STVCs and ASMFs, and *Nk4/Nkx2-5* represses *Tbx1/10* and *Ebf* in the SHP (Razy-Krajka et al., 2014; Wang et al., 2013). FGF-MAPK signaling is a key determinant of heart vs. ASM fate in cardiopharyngeal progenitors: it is necessary and sufficient to specify pharyngeal muscle identity at the expense of the alternative cardiac fate (Razy-Krajka et al., 2018). FGF-MAPK signaling is active in TVCs and subsequently maintained in STVCs and then ASMFs. This progressive restriction regulates the corresponding restricted expression of *Hand-r*, *Tbx1/10,* and *Ebf* to these cell types, in addition to a number of similarly patterned genes.

Single cell transcriptome profiling of individual FACS-purified cardiopharyngeal lineage cells identified comprehensive lists of genes associated with one of three distinct cardiopharyngeal fates: FHP, SHP, and ASM (Wang et al., 2017). The Wnt co-receptor *Lrp4/8* is a pan-cardiac marker expressed in both SHP and FHP at 20hpf. Additionally, the Wnt receptor *Frizzled4*, along with two Wnt ligands, *Wnt9b* and *Wnt10a*, are FHP-specific markers (Wang et al., 2017). Here we investigate the function of Tcf in the cardiopharyngeal mesoderm of *Ciona*. Since Wnt signal reception and binding of β-catenin converts Tcf from a repressor into an activator, we hypothesized that Tcf may be differentially activated in a cell type-specific manner during cardiac vs. pharyngeal muscle specification. Additionally, since several Wnt pathway components are pan-cardiac or FHP-specific molecular markers at later stages, we speculated that Wnt-Tcf activity may be further required specifically in heart progenitors to regulate a later aspect of cardiac differentiation and/or morphogenesis.

2. Results

2.1. Canonical Wnt pathway components are expressed in dynamic patterns during cardiopharyngeal development

The *Ciona robusta* genome encodes a single transcription factor of the Lef/Tcf family, *Cirobu.Tcf* (Stolfi et al., 2015; Yamada et al., 2003). *Tcf* mRNAs are maternally supplied and broadly expressed in early embryos (Imai et al., 2004; Squarzoni et al., 2011). At 20hpf, when heart progenitors are fate-restricted, *Tcf* transcripts are more abundant in heart precursors relative to ASMPs based on single-cell RNA sequencing analysis and whole mount in situ hybridization (Wang et al., 2017). We sought to determine when *Tcf* is zygotically up-regulated in the cardiopharyngeal lineage. We detected nascent *Tcf* transcription by in situ hybridization in the nuclei of late migratory TVCs in 10–12hpf tailbud embryos, consistent with previous microarray analyses (Fig. 1B, C; (Christiaen et al., 2008; Razy-Krajka et al., 2014)). This stage immediately precedes the first asymmetric TVC division, after which *Tcf* expression and ongoing transcription persists in both STVCs and FHPs as indicated by mRNA and nascent-RNA-specific probes (Fig. 1D, E).

Previous microarray profiling data indicated that several Wnt pathway genes are transcriptionally up-regulated in the cardiopharyngeal lineage (Christiaen et al., 2008; Razy-Krajka et al., 2014). We evaluated the lineage-specific expression patterns of these genes with in situ hybridization assays in TVCs (12hpf), in STVCs and FHPs after the first TVC division (14–15hpf), and in ASMFs, SHPs and FHPs after the STVC division (at 16hpf; Fig. 1B). Genes encoding the co-repressor *Tle*/*Groucho* (Fig. 1F-G) and the G-protein coupled receptors *Frizzled 4* (*Fzd4*) and *Frizzed 5/8* (*Fzd5/8*) are expressed in TVCs, among other tissues, at 12hpf. After the TVCs divide, *Fzd5/8* expression becomes asymmetric, and higher in the STVCs (Fig. 1H), and *Fzd4* expression was hardly detectable but also asymmetric and primarily observed in the FHPs (Fig. 1I). Indeed, single cell RNA sequencing analysis of cardiopharyngeal lineage cells isolated from 20 hpf larvae identified

Fzd4 as an FHP-specific marker, and here we show that FHP-specific expression can be observed as early as 16hpf, when both FHPs, SHPs and ASMFs are observed. Also at 16hpf, the expression of the Wnt inhibitor *Tiki* (Cruciat and Niehrs, 2013; Zhang et al., 2012), which was first detected in the migrating TVCs (Razy-Krajka et al., 2014), is restricted to ASMFs (Fig. 1J). *Dickkopf (Dkk)* encodes another secreted Wnt inhibitor, which is often activated by Wnt signaling itself (Cruciat and Niehrs, 2013; Niida et al., 2004), suggesting that *Dkk* expression is read-out of canonical Wnt activity. We observe that *Dkk* expression is more highly expressed in the secondary TVCs (Fig. 1K), suggesting asymmetric activation of canonical Wnt signaling in the STVCs.

To test whether *Dkk* expression is a reliable read-out of canonical Wnt signaling activity, we treated embryos with the GSK3 inhibitor 6-bromoindirubin-3-oxim (BIO), and observed ectopic up-regulation of *Dkk* in the entire trunk of the embryo, most notably in the mesenchyme, endoderm and sensory vesicle (Fig. 1L vs. 1M). *Dkk* is not

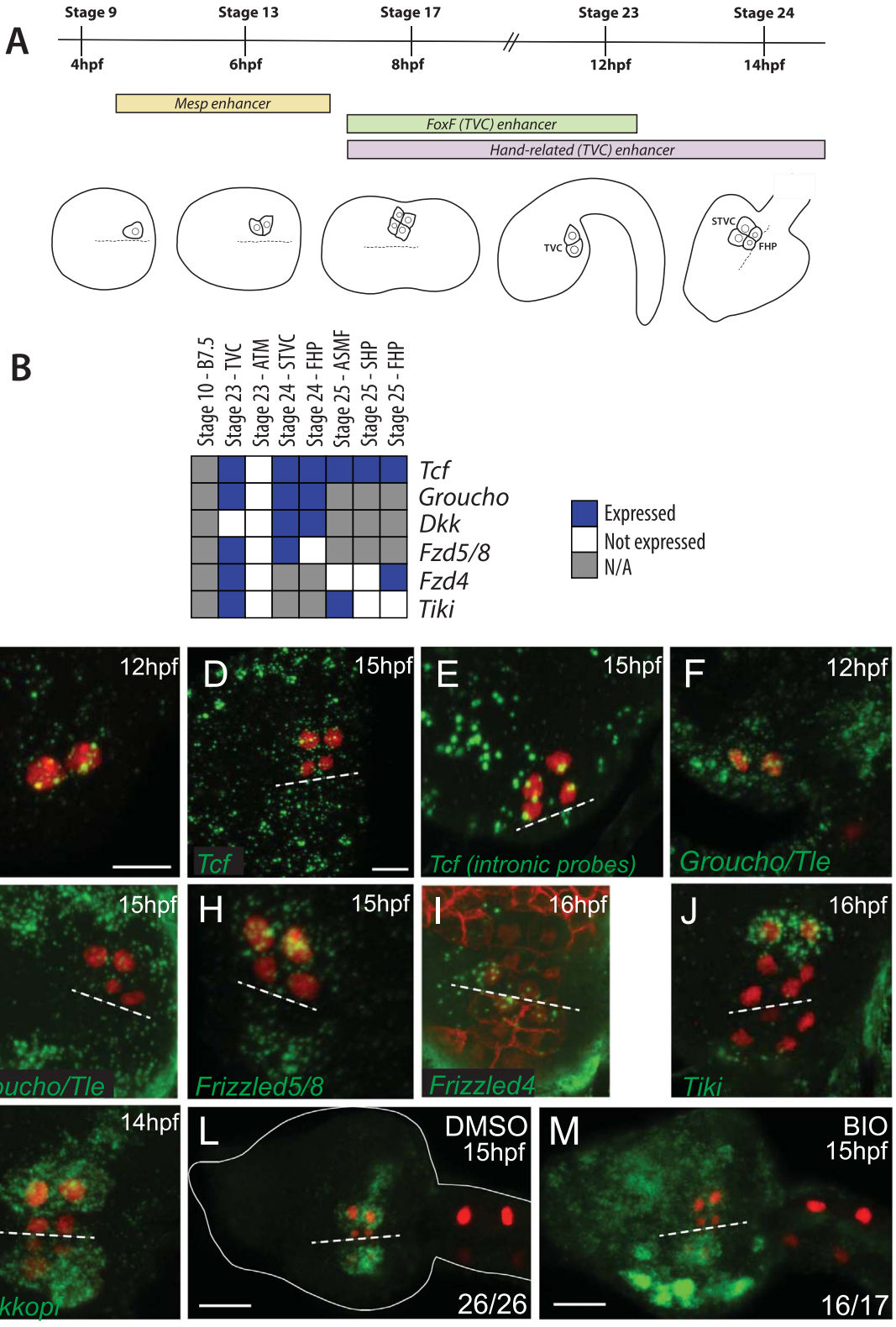

Fig. 1. Endogenous expression of Wnt pathway components in cardiopharyngeal progenitors. (A) Schema of the cardiopharyngeal lineage at five different developmental stages: (1) the B7.5 blastomere, (2) two founder cells born from a symmetric division of B7.5, (3) two newly born trunk ventral cells (TVCs) and two anterior tail muscle cells (ATMs) formed from an asymmetric division of the founder cells, (4) TVCs after migration into the trunk in the late tailbud embryo, and (5) two lateral secondary TVCs (STVCs) and two medial first heart precursors (FHPs) formed from an asymmetric division of the TVCs. One side of the bilaterally symmetric embryo is depicted, dotted lines represent the ventral midline. Embryonic stages are aligned with hours of development at 18 °C post fertilization (hpf) and the onset of drivers used in this study. (B) Heatmap summarizing in situ validated cell type-specific expression of Wnt components across the above developmental stages. (C) Representative expression pattern of *Tcf* in the two TVCs visualized with an anti-sense RNA probe by in situ hybridization in embryos 12hpf at 18 °C. TVCs and their progeny are marked by a nuclear-localized *H2B::mCherry* fluorescent reporter driven by *Mesp* and visualized by immunostaining. Anterior is to the left. Scale bar, 10 μM. (D) *Tcf* (KH.C6.71) expression in 15hpf larvae. *Tcf* is expressed in the two STVCs, the two FHPs, and in the trunk epidermis. The dotted line represents the ventral midline. Only one side of the embryo is electroporated due to left-right mosaicism. (E) Ongoing *Tcf* expression in a 15hpf larva visualized by intronic probes; nascent transcripts are observed in STVCs and FHPs. (F) Expression pattern of *Groucho/TLE* (KH.L96.11) in the two TVCs in 12hpf embryos and (G) in 15 hpf larvae. (H) Expression pattern of *Frizzled5/8* (KH.C9.260) in 15hpf larvae. *Fzd5/8* is asymmetrically expressed in STVCs at this stage. (I) Expression pattern of *Frizzled4* (KH.C6.162) in 16hpf larvae at 18 °C. TVCs and their progeny are marked with *H2B::mCherry* as well as membrane localized *CD4::mCherry* driven by *Mesp*; the mesenchyme is marked by *CD4::mCherry* driven by the *Twist* enhancer. Both sides of the larva are electroporated. *Fzd4* expression is restricted to FHPs at this stage. (J) Expression pattern of *Tiki* (KH.L170.89) at 16hpf at 18 °C, restricted to ASMFs at this stage. (K) *Dkk* (KH.L20.29) at 14hpf at 18 °C is asymmetrically expressed in STVCs at this stage. (L) *Dkk* expression in embryos incubated in seawater containing DMSO vs. (M) the GSK3 inhibitor BIO from 12 to 15 hpf. Three independent replicates were conducted for the treatments and scores were combined. Scale bar, 25 μM.

ectopically activated in FHPs, as it is normally expressed in these cells. However, it is possible that BIO treatment up-regulates *Dkk* expression levels in FHPs, as *Dkk* is normally expressed at lower levels in FHPs than in STVCs. While our qualitative in situ hybridization methods cannot detect this, we did not observe a striking up-regulation specifically in FHPs. In summary, the cardiopharyngeal precursors up-regulate *Tcf* right before they divide asymmetrically and express several components of the Wnt machinery, raising the possibility that *Tcf* may regulate the binary fate choice between STVC and FHP.

2.2. Lineage-specific Tcf perturbations do not affect STVC gene expression

Cirobu.Tcf has a conserved β-catenin binding domain at its N-terminus and a conserved DNA-binding high mobility group (HMG) domain (Fig. 2A; (Squarzoni et al., 2011)). To determine if Tcf is required for the expression of TVC-expressed genes, we expressed an active dominant-negative form of Tcf under the control of the *Mesp* promoter (*Mesp > Tcf$^{\Delta N}$::mCherry*; (Squarzoni et al., 2011)), which drives expression in the B7.5 blastomeres as early as the gastrula stage (Fig. 1A), and analyzed the expression of TVC markers *Hand-related* (Fig. 2B-C)), *Foxf* (Fig. 2D-E), and *Gata4/5/6* (Fig. 2F-G) in late tailbud embryos. This dominant-negative version of Tcf lacks the N-terminal β-catenin binding domain, and the design is widely used in functional studies to interfere with β-catenin-dependent Tcf activity (Molenaar et al., 1996). Electroporation of *Mesp > Tcf$^{\Delta N}$::mCherry* blocked both TVC migration and marker gene expression, preventing further analysis of later Tcf function during cardiopharyngeal fate specification (Fig. 2B-G). We reasoned that *Tcf$^{\Delta N}$* could be acting as a dominant repressor in this context, as there are conserved putative Tcf binding sites in the TVC-specific *Hand-r* enhancer. To circumvent this issue and interfere specifically with the β-catenin-dependent activator function of Tcf, we created a truncation of the Tcf protein to over-express only the N-terminal β-catenin binding domain fused to mCherry, thus mimicking the natural "passive" dominant negative Chibby (Takemaru et al., 2003), which competes with Tcf for β-catenin binding. To further test if a Tcf interaction with β-catenin is necessary for fate specification in cardiopharyngeal progenitors, we expressed this transgene (*Tcf^{Nterm}::mCherry*) specifically in the TVCs by using the TVC-specific *Foxf* enhancer, which becomes active in newly born TVCs in initial tailbud embryos (Fig. 1A), and performed in situ hybridization assays for STVC and ASM markers. TVC-specific expression of *Tcf^{Nterm}::mCherry* blocked *Dkk* expression in the STVCs (Fig. 2H vs. 2I). However, we did not observe robust down-regulation of either *Hand-r* or *Tbx1/10* in embryos expressing this transgene when compared to control embryos expressing *Foxf(TVC) > mCherry* (not shown).

To circumvent technical difficulties inherent to misexpressing dominant negative mutant forms of Tcf, we developed complementary reagents for loss-of-function perturbations. We started with a tissue-specific microRNA-based RNAi approach (Haley et al., 2008) and generated short hairpins mimicking the microRNA miR-2213 from *Ciona robusta* (Shi et al., 2009; Wang et al., 2013). We repurposed this hairpin structure by incorporating it into a plasmid-based short hairpin microRNA (shmiR) backbone also designed to mimic the endogenous pri-miR-2213, into which we cloned several short hairpins targeting the *Tcf* mRNA. We expressed these hairpins lineage-specifically with the *Mesp* enhancer, and validated them individually and pairwise by co-expression with a GFP::Tcf fusion protein (*Mesp > GFP::Tcf*). As a proxy for effective gene silencing, we quantified relative fluorescence levels of the Mesp > GFP::Tcf sensor normalized to fluorescence driven by *Mesp > H2B::mCherry* (Supplemental Fig. 1). We then concatemerized the two most efficient hairpins into a shmiR expression plasmid. We expressed these Tcf-specific shmiRs with the TVC-specific *Hand-r* enhancer, but did not observe differences in *Hand-r* or *Tbx1/10* expression based on in situ hybridization assays when compared to concatemerized control hairpins targeting the gene encoding firefly *luciferase*. However, we did observe marked down-regulation of *Dkk* expression by targeted expression of Tcf shmiRs (Fig. 2J vs. 2K). Taken together, these results suggest that *Tcf*-mediated transcriptional inputs operate in parallel to the pathway(s) regulating *Hand-r* and *Tbx1/10* expression in STVCs.

To better understand the potential dominant negative nature of *Mesp > Tcf$^{\Delta N}$::mCherry* which blocked TVC migration and specification, we attempted to confirm this result by evaluating effects on migration upon over-expression of *Mesp > Tcf^{Nterm}::mCherry* or Mesp-driven Tcf shmiRs (Supplemental Fig. 2). Neither Mesp-driven Tcf^{Nterm} nor Tcf shmiRs blocked TVC migration, indicating that the effects observed with *Mesp > Tcf$^{\Delta N}$::mCherry* may reflect dominant repression via Tcf binding sites, such as those found in the *Hand-related* enhancer. However, since we could not confirm the efficacy of *Mesp*-driven Tcf^{Nterm} or Tcf shmiRs at the earliest stages, we cannot formally rule out the possibility of a role for maternal Tcf proteins beyond *Lhx3* and *Mesp* activation in the B7.5 lineage. Addressing this possibility will await the development of refined tools for loss-of-function assays of maternal protein at later embryonic stages.

2.3. Transcriptome profiling in Tcf loss-of-function conditions reveals that Tcf does not regulate early cardiopharyngeal fate specification

To further assay Tcf function independently of its hypothetical role in mediating canonical Wnt signaling, we generated the reagents for independent *Tcf* loss-of-function by targeting the *Tcf* locus with CRISPR/Cas9-mediated mutagenesis. We used two sgRNAs targeting the predicted promoter and two sgRNAs targeting the first exon, the latter with estimated mutagenesis efficiencies of 30.1% and 43.6% (Lef1.1 and Lef1.2 sgRNAs, respectively) according to prior evaluation (Gandhi et al., 2017; Stolfi et al., 2014). For the *Tcf^{CRISPR}* condition, we electroporated fertilized eggs with these four sgRNA-expressing constructs driven by the ubiquitous *U6* promoter which is active at the 16-cell stage (Pickett and Zeller, 2018; Stolfi et al., 2014), along with

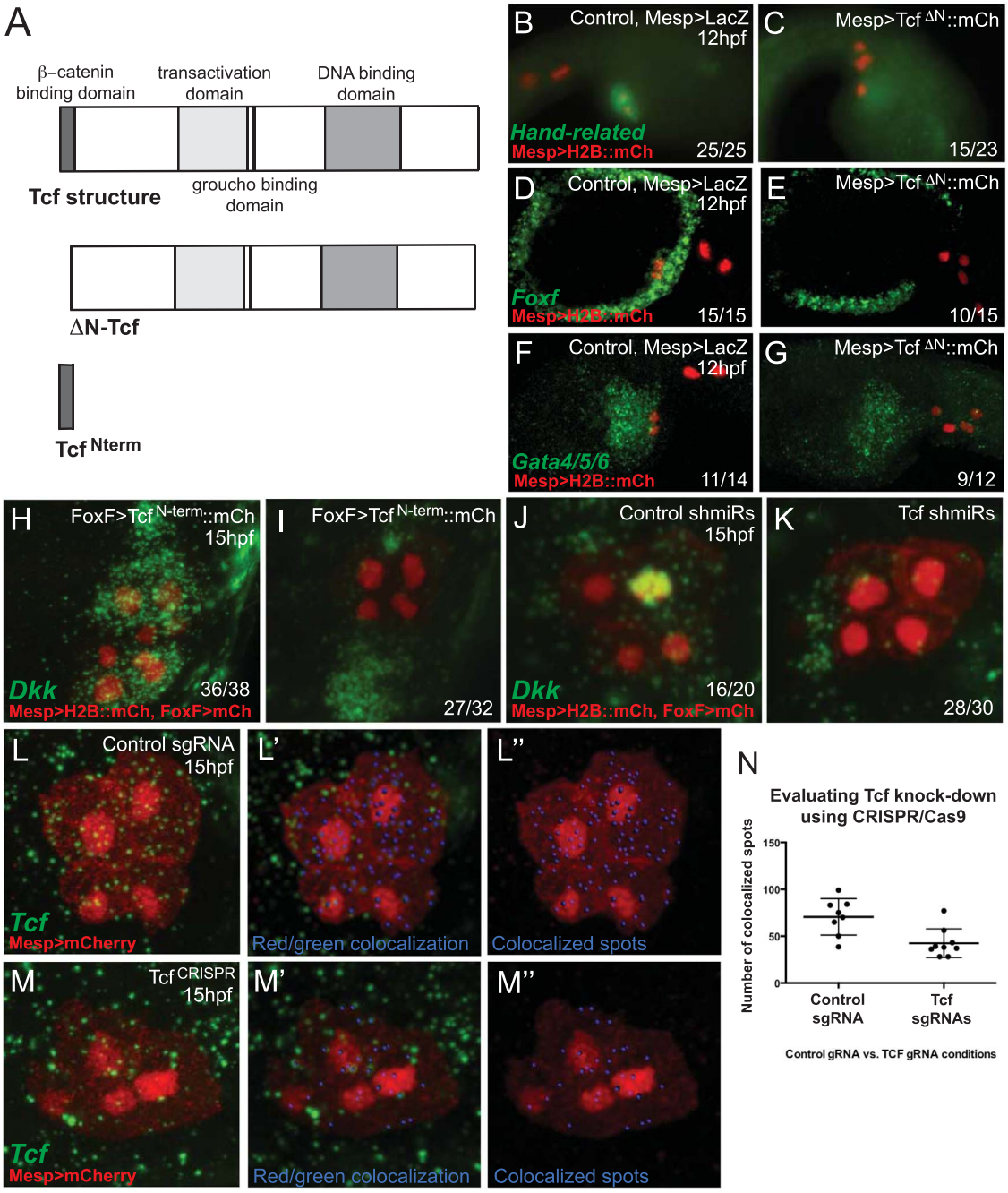

Fig. 2. Functional perturbations to study Wnt-Tcf signaling. **(A)** Schematic representation of Cirobu.Tcf. Rectangles represent conserved protein domains. The β-catenin binding domain, transactivation domain, groucho binding domain, and DNA binding domain are indicated. $Tcf^{\Delta N}$ lacks the β-catenin binding domain; Tcf^{Nterm} is an over-expression of the β-catenin binding domain. **(B-K)** Expression analysis by in situ hybridization in control vs. perturbation. TVCs and their progeny are marked by a nuclear localized mCherry fluorescent reporter driven by *Mesp*. TVC-specific over-expression of dominant-negative Tcf ($Tcf^{\Delta N}$) blocks TVC migration and induces loss of **(B-C)** *Hand-r* expression, **(D-E)** *Foxf* expression and **(F-G)** *Gata4/5/6* expression in TVCs. Two replicates were performed for each and scores were combined. **(H-I)** TVC-specific over-expression of Tcf^{Nterm} blocks *Dkk* expression in TVC progeny. Four replicates were performed and scores were combined. **(J-K)** TVC-specific over-expression of Tcf shmiRs blocks *Dkk* expression in TVC progeny. Two replicates were performed and scores were combined. **(L-M)** *Tcf* expression visualized with an anti-sense RNA probe by in situ hybridization in control vs. Tcf^{CRISPR} conditions. TVCs and their progeny are marked by an mCherry fluorescent reporter driven by Mesp. **(L'-M')** A new channel (blue) was created for red/green colocalization in a defined region of interest and **(L''-M'')** the punctate expression was defined as spots in the colocalization channel as a proxy for *Tcf* expression within the TVC lineage, quantified in **(N).**

Mesp > nls::Cas9::nls as described (Gandhi et al., 2017). Mesp-driven expression of the Cas9 endonuclease enables targeting of the *Tcf* locus specifically in the B7.5 lineage, and we previously estimated that mutagenesis occurs during gastrulation, before 8 hpf (Stolfi et al., 2014). For stage-matched control samples, we used a guide RNA targeting a sequence absent from the *Ciona* genome (Stolfi et al., 2014). To validate the efficacy of the *Tcf* knock-down, we used in situ hybridization assays to detect endogenous *Tcf* expression levels in control vs. Tcf^{CRISPR} conditions. We generated semi-quantitative estimates of *Tcf* expression by counting *Tcf*+ fluorescent dots in the cardiopharyngeal lineage segmented using *Mesp > mCherry*, with the Imaris software (Fig. 2L-M). Using these estimates as a proxy for transcript abundance, we estimated a knock-down efficiency of ~40% (Fig. 2N; unpaired *t*-test, $p = 0.0046$). This is likely an underestimate, as transcripts with CRISPR/Cas9-induced mutations may be detected by in situ hybridization irrespective of whether they produce a

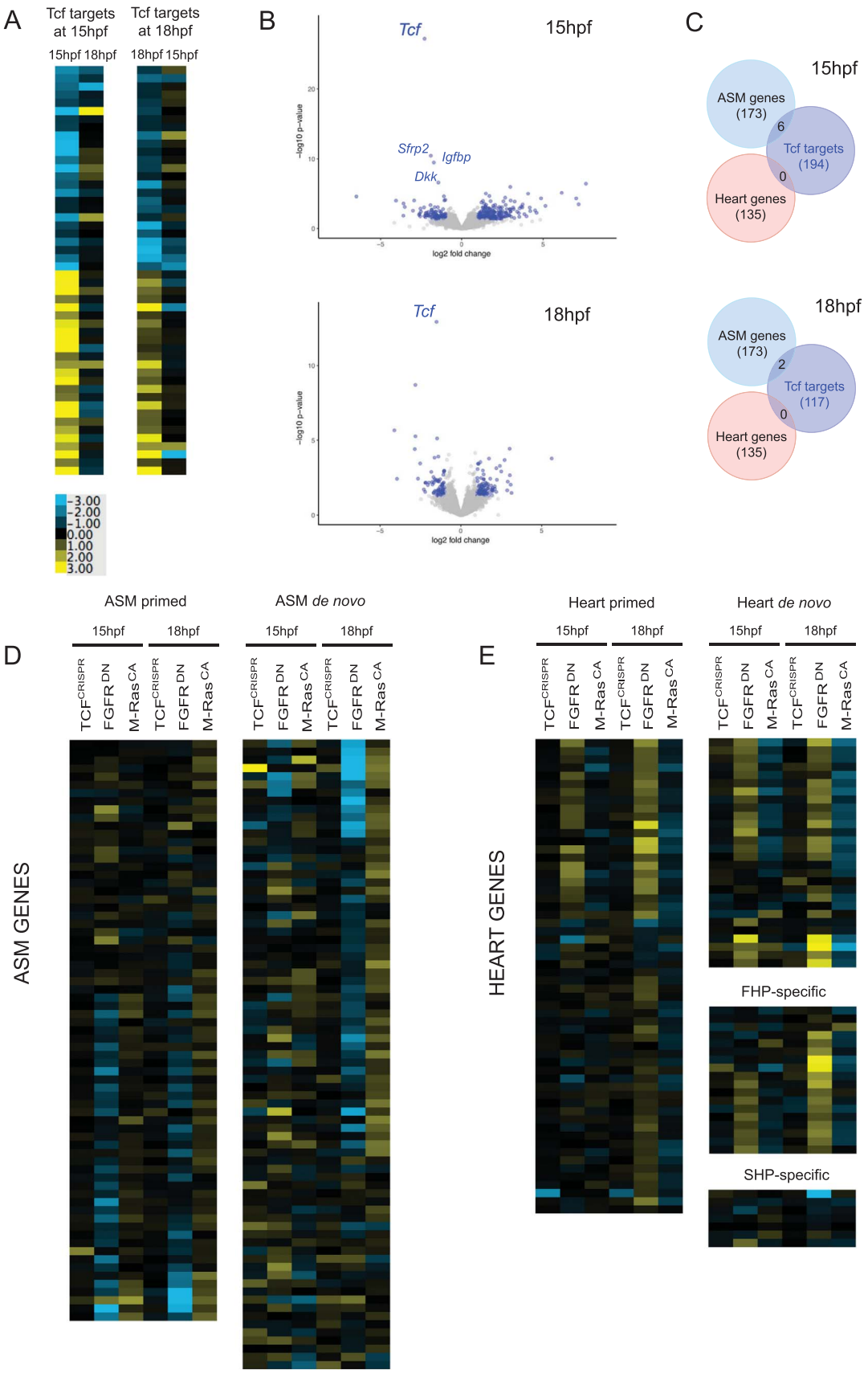

Fig. 3. Transcriptome profiling reveals that *Tcf* is dispensable for early cardiopharyngeal fate specification. **(A)** Heatmap showing log fold changes at 15hpf vs. 18hpf of significantly down-regulated (blue) and up-regulated (yellow) Tcf targets at 15hpf and 18hpf; most targets are significantly regulated at either 15hpf or 18hpf, but not both. **(B)** Volcano plot showing fold-change vs. significance on the x and y axes, respectively at 15hpf and 18hpf. Significantly regulated genes are shown in blue and the rest are shown in gray. **(C)** Euler diagram representing the overlap between Tcf targets and ASM genes and heart genes. **(D)** Heatmap showing log fold changes at 15hpf and 18hpf of primed and *de novo* ASM genes in Mesp > Cas9/Tcf ^{CRISPR}, Hand-related(TVC) > Fgfr^{DN}, and FoxF(TVC) > M-Ras^{CA} perturbations. **(E)** Heatmap showing log fold changes at 15hpf and 18hpf of primed and *de novo* heart genes, FHP-specific genes, and SHP-specific genes, in Tcf ^{CRISPR}, Fgfr^{DN}, and M-Ras^{CA} perturbations.

functional protein, but on the other hand, CRISPR/Cas9-mediated mutagenesis would alter neither maternal transcripts nor maternal proteins, which may remain in the cells. Nevertheless, we reasoned that our CRISPR/Cas9 reagents efficiently interfere with zygotic *Tcf* activity, which we detected starting in late tailbud embryos.

To more systematically characterize the potential effects of *Tcf* on cardiopharyngeal gene regulation, we dissociated larvae at 15- and 18hpf and profiled the transcriptomes of FACS-purified cardiopharyngeal cells expressing control versus Tcf^{CRISPR} targeting reagents. These two developmental time points follow each of the asymmetric divisions that segregate the heart and ASM transcriptional programs. Using standard procedures for differential gene expression analysis using RNA-seq, we identified 194 and 117 differentially expressed genes between control and Tcf^{CRISPR} conditions in the 15- and 18hpf data sets, respectively (cutoff p-value < 0.01; Fig. 3A-B). *Tcf* was the most significantly down-regulated gene in the Tcf^{CRISPR} condition compared to control, confirming the efficacy of our loss-of-function assay. Generally, the most significantly up-regulated and down-regulated genes differed between 15 and 18hpf (Fig. 3A-B). Notwithstanding, we reasoned that if *Tcf* regulates heart vs. pharyngeal muscle fate choices, there should be an enrichment of genes associated with heart vs. ASM fate among the regulated Tcf targets at one or both time points. However, neither cardiac nor ASM markers, defined by single cell RNA-seq analysis, were enriched among candidate Tcf targets (Fig. 3C; (Wang et al., 2017)). In bulk RNA-seq experiments, inhibiting FGF-MAPK signaling by lineage-specific expression of a dominant negative form of fibroblast growth factor receptor (*Hand-r(TVC) > Fgfr*^{DN}) down-regulates molecular markers associated with ASM fate, and up-regulates those associated with cardiac fate (Wang et al., 2017). Conversely, a gain-of-function of FGF-MAPK activity by expressing a constitutively active form of M-Ras (*FoxF(TVC) > M-Ras*^{CA}) down-regulates cardiac markers, while up-regulating ASM markers. These analyses reinforce the importance of FGF-MAPK signaling as a molecular switch regulating heart vs. ASM fate (Razy-Krajka et al., 2018; Wang et al., 2017). In contrast to unambiguous up- or down-regulation induced by targeted perturbations of FGF-MAPK signaling, differential expression was barely detectable in Tcf^{CRISPR} conditions of both ASM (Fig. 3D) and heart markers (Fig. 3E). This analysis supports the notion that *Tcf* operates primarily in parallel to the main pathways regulating early cardiac vs. pharyngeal muscle specification in *Ciona*.

2.4. *Tcf up-regulates the expression of secreted Wnt antagonists*

The top three genes down-regulated by Tcf^{CRISPR} at 15hpf were *Dkk*, an *Igfbp* homolog (KH.C4.404), and *Sfrp2*. *Dkk* and *Sfrp2* are established secreted antagonists of the canonical Wnt pathway (Kawano and Kypta, 2003), and *Igfbp-4* has also been implicated in Wnt antagonism (Zhu et al., 2008). Moreover, these three genes have all been reported to inhibit Wnt signaling specifically during heart development (David et al., 2008; Schmeckpeper et al., 2015; Zhu et al., 2008). We analyzed the expression of these genes with in situ hybridization assays at 15hpf, the time point at which they are differentially expressed in control vs. Tcf^{CRISPR} conditions. *Dkk* and *Igfbp* both show restricted expression patterns in the STVCs, with lower levels detected in the FHPs (Fig. 1K, Fig. 4B). *Sfrp2*, however, is expressed at higher levels in the FHP at 15pf (Fig. 4A), and indeed is an FHP-specific marker at 14hpf based on single-cell RNA sequencing analysis (Wang et al., 2017). Although, we did not investigate the potential function of these three Wnt antagonists, we speculate that they may contribute to maintaining canonical Wnt signaling inactivity, while preserving the ability of cardiopharyngeal lineage cells to respond to Wnt in subsequent developmental steps (see below).

2.5. *Wnt-Tcf signaling in late stages of heart organogenesis*

Since *Tcf* and the Wnt co-receptor *Lrp4/8* are expressed at higher levels in heart precursors relative to ASMPs, and Wnt ligands along with the *Fzd4* receptor are FHP-specific markers (Wang et al., 2017), we then asked if Wnt signaling regulates a later aspect of cardiopharyngeal development specifically in FHPs. Both FHPs and STVC-derived SHPs contribute to the juvenile heart; the latter can be marked by the expression of the STVC-specific *Tbx1/10* enhancer and are typically arranged at the periphery of the heart, whereas FHP derivatives are more centrally located and express the late cardiac differentiation marker *Mhc2*. To determine if *Tcf* has a role during late cardiac differentiation or morphogenesis, we analyzed the proportion of *Mhc2*-expressing cells, as well as the proportion of SHPs in the hearts of 2 day old post-metamorphic juveniles in control vs. Tcf^{CRISPR} conditions (Fig. 5A-J). In control vs. Tcf^{CRISPR} juveniles, the proportion of *Mhc2*-expressing cells in the heart was on average 29.9% (SD ± 6.6%) vs. 19.7% (SD ± 13.4%) (unpaired *t*-test, p = 0.09), and the proportion of SHPs in the heart was 15% (SD ± 5.3%) vs. 10.4% (SD ± 6.8%)

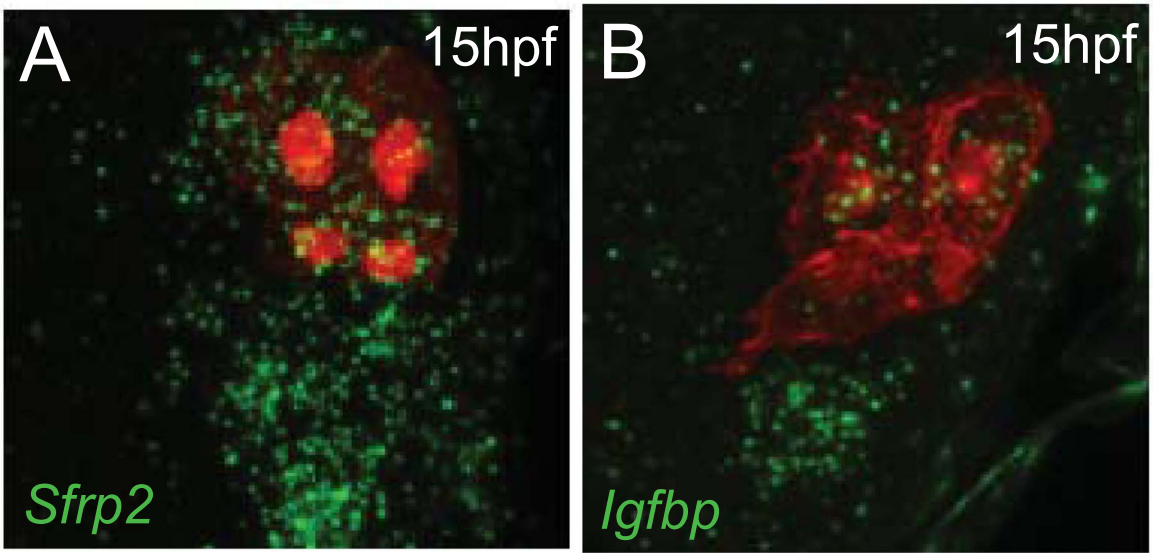

Fig. 4. Expression of Tcf targets *Sfrp2* and *Igfbp* in STVCs and FHPs. **(A)** Expression analysis by in situ hybridization of Tcf targets *Sfrp2* and **(B)** *Igfbp*, at 15hpf. TVCs and their progeny are marked by nuclear localized and membrane localized mCherry fluorescent reporters driven by *Mesp*.

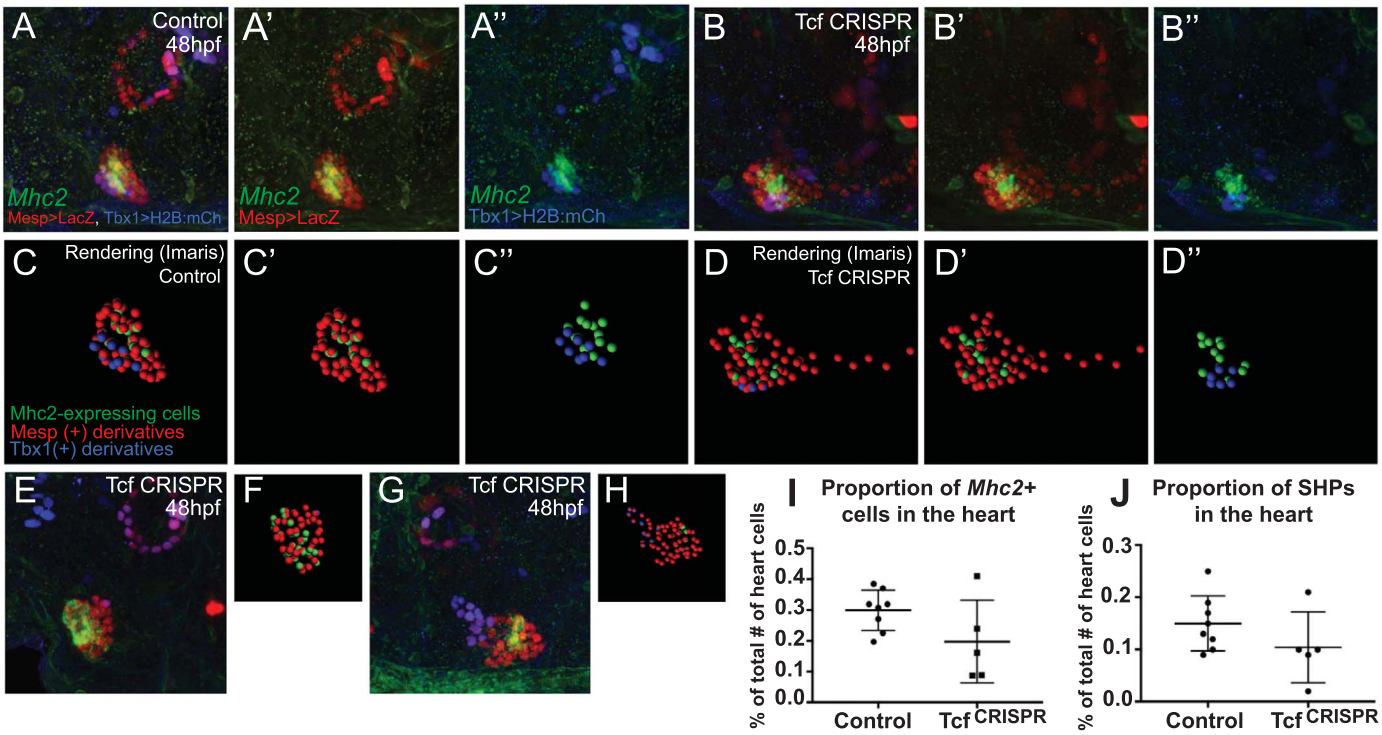

Fig. 5. Investigating a potential role for Tcf during late cardiac morphogenesis. **(A)** *Mhc2* expression visualized by in situ hybridization in juvenile hearts. TVC derivatives are marked with a nuclear localized LacZ reporter driven by *Mesp* - the heart as well as ASM ring are observed. STVC derivatives are marked with a histone localized mCherry reporter driven by a STVC-specific *Tbx1* enhancer - a subset of cells in the heart (SHP derivatives) and ASM ring are labeled. **(B)** *Mhc2* expression in Tcf ^{CRISPR} juvenile hearts. Same labelling scheme as in (A). **(C-D)** Rendering in Imaris of representative control vs. Tcf ^{CRISPR} juvenile hearts. Mesp+ and Tbx1/10 + nuclei were identified as spots, and the colocalization function was used to count the number of *Mhc2* + spots. **(E, G)** Additional examples of Tcf ^{CRISPR} juvenile heart phenotypes, Imaris renderings in **(F, H)**, proportions quantified in **(I, J)**.

(unpaired *t*-test, p = 0.2), respectively. We reasoned that this variability could be due to technical factors (transgenesis via electroporation of CRISPR reagents), or possibly because *Tcf* can act as both a repressor and an activator, thus resulting in a range of phenotypes at the juvenile stage. This suggests that Wnt-Tcf signaling is dispensable for early FHP specification but our observations are consistent with a later role for Wnt/Tcf signaling in cardiac organogenesis and/or cardiomyocyte differentiation.

3. Discussion

Here, we show that *Tcf* and several Wnt pathway components are dynamically expressed in multipotent cardiopharyngeal progenitors and throughout the developmental transitions that specify cardiac vs. pharyngeal muscle fate. We developed molecular tools to study the function of the *Ciona robusta* Lef/Tcf homolog and other Wnt signaling pathway components using a novel dominant-negative, tissue-specific RNAi and CRISPR/Cas9 reagents. While the *Tcf^{Nterm}* construct links Tcf to Wnt/β-catenin signaling, the other molecular tools used to achieve Tcf knock-down could reflect β-catenin-independent roles for Tcf. Extensive functional analyses failed to demonstrate a clear effect of Wnt-Tcf signaling perturbations on cardiac and/or pharyngeal muscle gene expression, suggesting that Wnt-Tcf signaling is largely dispensable for early fate specification in cardiopharyngeal progenitors. By contrast, our initial characterization of latter cardiac phenotypes following inhibition of Tcf does not rule out a role for Wnt-Tcf signaling in heart organogenesis.

Recent studies indicated that differential FGF-MAPK signaling is active in multipotent cardiopharyngeal progenitors and acts as the predominant molecular switch to specify cardiac vs. pharyngeal muscle in Ciona (Razy-Krajka et al., 2018; Wang et al., 2017). Notably, the expression of *Tcf* itself, and that of other Wnt signaling pathway components analyzed in this study depend upon regulation of FGF-MAPK signaling. This suggested that Wnt signaling could be mediating some of the effects of FGF-MAPK on cardiopharyngeal fate specification, as FGF and Wnt signaling pathways interact during SHF development in the mouse (e.g. (Cohen et al., 2007)). Functional assays using reagents designed to interfere with Tcf repressor or β-catenin-dependent activator functions produced somewhat variable effects, inconsistent with a major role for Wnt-Tcf signaling in early heart vs. pharyngeal muscle specification. Besides experimental variability, we reason that these conflicting observations could hint at a subtle role for the dual regulator *Tcf* as a safeguard mechanism to ensure the robust segregation of opposing transcriptional programs. For instance, the observation that loss of Tcf function down-regulated the expression of several secreted Wnt antagonists suggested a mechanism whereby cells are competent but prevented to activate Wnt signaling during early fate specification. Future analyses using precise genetic reagents and quantitative assays will be necessary to explore of potential role for Tcf in fostering robustness to the cardiopharyngeal fate choices.

The absence of a clear role for Wnt-Tcf signaling in early heart vs. pharyngeal muscle fate specification in *Ciona* contrasts with reports using vertebrate model systems, which invoked a negative effect of canonical Wnt on cardiac progenitor specification (Marvin et al., 2001; Schneider and Mercola, 2001; Tzahor and Lassar, 2001). However, the effects of canonical Wnt signaling on heart development depend upon the developmental window: Wnt signaling promotes early specification of the cardiogenic mesoderm before gastrulation in zebrafish and in mouse embryonic stem cells (Dohn and Waxman, 2012; Naito et al., 2006; Ueno et al., 2007), and later proliferation of second heart field progenitors ((Ai et al., 2007; Cohen et al., 2007; Kwon et al., 2007; Lin et al., 2007); reviewed in Tzahor (2007)). From that standpoint, we note that early perturbation of Tcf function with the active dominant-negative Tcf$^{\Delta N}$ blocked TVC induction. Indeed, previous studies

showed that β-catenin activity is required for *Mesp* expression in the B7.5 lineage by activating its upstream regulator Lhx3 (Christiaen et al., 2009; Satou et al., 2004).

Finally, whereas our observations suggest that Wnt-Tcf signaling is dispensable for early fate specification in the cardiopharyngeal lineage of *Ciona*, it may be required post-hatching for proper heart morphogenesis during metamorphosis. For instance, our observations point to a potentially intriguing parallel with the roles of canonical Wnt signaling in second heart field development and cardiomyocyte differentiation.

Looking forward, further development of measurable parameters for the precise evaluation of late morphological phenotypes will foster a better understanding of cardiac organogenesis, and the potential conserved roles played by Wnt-Tcf signaling.

4. Materials and methods

4.1. Animals, embryo preparation, and electroporation

Wild *Ciona robusta* adults were obtained from California. Isolation of gametes, fertilization, dechorionation, and electroporation of plasmid DNA were performed as described (Christiaen et al., 2009). Fluorescent reporters were electroporated at 10–50 μg per construct, experimental perturbations at 50–70 μg per construct, Mesp > nls:Cas9:nls at 35 μg, and sgRNAs at 25 μg each. Embryonic time points are indicated at hours post-fertilization (hpf) for development at 18 °C.

4.2. Pharmacological treatments

6-bromoindirubin-3′-oxime (BIO) was used at a final concentration of 2.5 μM in seawater. Embryos were bathed in treatment from 12 to 15hpf and fixed for analysis at 15hpf.

4.3. Molecular cloning

Ptyr > Ci-Tcf$^{\Delta N1}$::mCherry was kindly provided by Antonietta Spagnuolo; it was originally cloned by PCR amplification using two oligonucleotides (*N1F* and *N1R*) from a plasmid containing the full *Ci-Tcf* coding sequence (Squarzoni et al., 2011). *Ptyr > Ci-Tcf$^{\Delta N1}$::mCh* was digested with Not1/Blp1 and the ptyr enhancer was replaced with either the Mesp enhancer or the Foxf minimal TVC enhancer fused to the basal promoter of the gene *Friend of Gata* (bpFOG). Tcf^{Nterm} was digested from the construct *Mesp > Tcf^{Nterm}::LacZ::GFP* using Not1/Spe1 to create *Mesp > Tcf^{Nterm}::mCherry*.

4.4. Construction of short hairpin RNAs targeting Tcf (Tcf shmiRs)

We generated short hairpins mimicking the microRNA miR-2213 from C*iona robusta* (Shi et al., 2009; Wang et al., 2013). We incorporated this hairpin structure into a plasmid-based shmiR backbone designed to mimic the endogenous pri-miR-2213. The sequence of the shmiR cassette is as follows: aaa gcggccgc aaa gctagca taa tga acttcgtggccgtcgatcgtttaaagggaggtagtgaggtacctctagtggatcc [cgcggcgctaggttcgtttaatggtctaaaaatcaGagcgtttagt**GTTTG**gagaccgagagagggtctcactaa aactgcgcttattatcttctacgaacctgtaagtggc] agatct ggccgca ctcgag tttg atgaattccagctgagcg. Into this cassette, we cloned short hairpins targeting *Tcf* mRNA using BsaI digestion, and we expressed these hairpins downstream of the *Mesp* enhancer. After validation using a GFP::Tcf reporter (Supplemental Fig. 1, and described within), we concatemerized the two most efficient hairpins (Tcf shmiR 'C' and 'F') into a microRNA expression plasmid. Control shmiR plasmids were designed to contain hairpins targeting the gene encoding firefly *luciferase*.

4.5. FACS and RNA extraction

Fertilized eggs were electroporated with Mesp > tagRFP, Hand-r > tagBFP and

MyoD > GFP at 50 μg for each construct. Larvae were dissociated as previously described (Christiaen et al., 2009). FACS was performed on a BD FACS Aria cell sorter as previously described (Wang et al., 2018). RFP+/BFP+ cells were co-selected, and GFP+ mesenchymal cells were counter-selected. RNA extraction was performed using the RNAqueous-Micro RNA extraction kit (ThermoFisher).

4.6. RNA sequencing

cDNA synthesis was performed for two replicates of each condition at each developmental time point (Control sgRNA and Tcf^{CRISPR}, 15hpf and 18hpf) and sequencing libraries were prepared as previously described (Wang et al., 2018). Libraries were sequenced by Illumina HiSeq. 2500, single-end 50 bp reads were obtained, and sequenced reads were mapped to the *Ciona robusta* genome using TopHat 2.0.12.

4.7. Fluorescent in situ hybridization and immunohistochemistry

DIG-labeled RNA probes were created using anti-DIG-POD Fab fragments (Roche). Detection was achieved using the tyramide signal amplification (TSA) fluorescein system (Perkin Elmer). Samples were fixed in MEM-PFA with Tween-20 (0.05%) for 2–3 h at room temperature, gradually dehydrated using a methanol/PBS-Tween series of washes (33%, 50%, 75%), and stored at −20 °C. They were then rehydrated gradually using a methanol/PBS-Tween series, and whole mount fluorescent in situ hybridization was performed as previously described (Wang et al., 2013; Razy-Krajka et al., 2014). For immunohistochemistry, samples were blocked in Tris-NaCl-Blocking buffer (Blocking Reagent, PerkinElmer) for 2–4 h preceding primary antibody incubation and 1 h preceding secondary antibody incubation. Antibody solutions were prepared in Tris-NaCl-Blocking buffer and incubated for 1–2 h at room temperature, followed by an overnight incubation at 4 °C. mCherry was detected using an anti-mCherry rabbit polyclonal antibody (1:500; Biovision) and LacZ was detected using an anti- β-galactosidase mouse monoclonal antibody (1:500; Promega). Primary antibodies were coupled with Alexa 568 and Alexa 647 (Invitrogen) and incubated at 2–3 h at room temperature or overnight at 4 °C. Antibody washes were performed using Tris-NaCl-Tween buffer, samples were mounted in Prolong Gold (Molecular Probes), and stored at 4 °C.

4.8. Microscopy and analysis

Phenotypic scoring analysis was conducted under a DM2500 epifluorescent microscope (Leica Microsystems) and confocal imaging was performed using a TCS SP8 X inverted confocal microscope (Leica Microsystems).

Acknowledgements

We thank Antonietta Spagnuolo for kindly sharing constructs and we thank Dylan Iannitelli for technical assistance. This work was funded by an NIH/NHLBI R01 award HL108643 to L.C., a trans-Atlantic network of excellence award 15CVD01 from the Leducq Foundation to L.C., and award 5T32HD007520-14 to N.K. as part of the New York University Developmental Genetics program.

Appendix A. Supporting information

Supplementary data associated with this article can be found in the online version at doi:10.1016/j.ydbio.2018.12.018.

References

Ai, D., Fu, X., Wang, J., Lu, M.-F., Chen, L., Baldini, A., Klein, W.H., Martin, J.F., 2007. Canonical Wnt signaling functions in second heart field to promote right ventricular growth. Proc. Natl. Acad. Sci. USA 104, 9319–9324.

Beh, J., Shi, W., Levine, M., Davidson, B., Christiaen, L., 2007. FoxF is essential for FGF-induced migration of heart progenitor cells in the ascidian Ciona intestinalis. Development 134, 3297–3305.

Bodmer, R., Venkatesh, T.V., 1998. Heart development in Drosophila and vertebrates: conservation of molecular mechanisms. Dev. Genet. 22, 181–186.

Buckingham, M., Meilhac, S., Zaffran, S., 2005. Building the mammalian heart from two sources of myocardial cells. Nat. Rev. Genet. 6, 826–835.

Chen, L., Fulcoli, F.G., Tang, S., Baldini, A., 2009. Tbx1 regulates proliferation and differentiation of multipotent heart progenitors. Circ. Res. 105, 842–851.

Christiaen, L., Davidson, B., Kawashima, T., Powell, W., Nolla, H., Vranizan, K., Levine, M., 2008. The transcription/migration interface in heart precursors of Ciona intestinalis. Science 320, 1349–1352.

Christiaen, L., Stolfi, A., Davidson, B., Levine, M., 2009. Spatio-temporal intersection of Lhx3 and Tbx6 defines the cardiac field through synergistic activation of Mesp. Dev. Biol. 328, 552–560.

Cohen, E.D., Tian, Y., Morrisey, E.E., 2008. Wnt signaling: an essential regulator of cardiovascular differentiation, morphogenesis and progenitor self-renewal. Development 135, 789–798.

Cohen, E.D., Wang, Z., Lepore, J.J., Lu, M.M., Taketo, M.M., Epstein, D.J., Morrisey, E.E., 2007. Wnt/beta-catenin signaling promotes expansion of Isl-1-positive cardiac progenitor cells through regulation of FGF signaling. J. Clin. Investig. 117, 1794–1804.

Cruciat, C.-M., Niehrs, C., 2013. Secreted and transmembrane wnt inhibitors and activators. Cold Spring Harb. Perspect. Biol. 5, a015081.

David, R., Brenner, C., Stieber, J., Schwarz, F., Brunner, S., Vollmer, M., Mentele, E., Müller-Höcker, J., Kitajima, S., Lickert, H., Rupp, R., Franz, W.-M., 2008. MesP1 drives vertebrate cardiovascular differentiation through Dkk-1-mediated blockade of Wnt-signalling. Nat. Cell Biol. 10, 338–345.

Davidson, B., Levine, M., 2003. Evolutionary origins of the vertebrate heart: specification of the cardiac lineage in Ciona intestinalis. Proc. Natl. Acad. Sci. USA 100, 11469–11473.

Davidson, B., Shi, W., Beh, J., Christiaen, L., Levine, M., 2006. FGF signaling delineates the cardiac progenitor field in the simple chordate, Ciona intestinalis. Genes Dev. 20, 2728–2738.

Davidson, E.H., Erwin, D.H., 2006. Gene regulatory networks and the evolution of animal body plans. Science 311, 796–800.

Delsuc, F., Brinkmann, H., Chourrout, D., Philippe, H., 2006. Tunicates and not cephalochordates are the closest living relatives of vertebrates. Nature 439, 965–968.

Dohn, T.E., Waxman, J.S., 2012. Distinct phases of Wnt/β-catenin signaling direct cardiomyocyte formation in zebrafish. Dev. Biol. 361, 364–376.

Gandhi, S., Haeussler, M., Razy-Krajka, F., Christiaen, L., Stolfi, A., 2017. Evaluation and rational design of guide RNAs for efficient CRISPR/Cas9-mediated mutagenesis in Ciona. Dev. Biol. 425, 8–20.

Gessert, S., Kühl, M., 2010. The multiple phases and faces of wnt signaling during cardiac differentiation and development. Circ. Res. 107, 186–199.

Haley, B., Hendrix, D., Trang, V., Levine, M., 2008. A simplified miRNA-based gene silencing method for Drosophila melanogaster. Dev. Biol. 321, 482–490.

Harel, I., Nathan, E., Tirosh-Finkel, L., Zigdon, H., Guimarães-Camboa, N., Evans, S.M., Tzahor, E., 2009. Distinct origins and genetic programs of head muscle satellite cells. Dev. Cell 16, 822–832.

Imai, K.S., Hino, K., Yagi, K., Satoh, N., Satou, Y., 2004. Gene expression profiles of transcription factors and signaling molecules in the ascidian embryo: towards a comprehensive understanding of gene networks. Development 131, 4047–4058.

Kawano, Y., Kypta, R., 2003. Secreted antagonists of the Wnt signalling pathway. J. Cell Sci. 116, 2627–2634.

Kwon, C., Arnold, J., Hsiao, E.C., Taketo, M.M., Conklin, B.R., Srivastava, D., 2007. Canonical Wnt signaling is a positive regulator of mammalian cardiac progenitors. Proc. Natl. Acad. Sci. USA 104, 10894–10899.

Lescroart, F., Chabab, S., Lin, X., Rulands, S., Paulissen, C., Rodolosse, A., Auer, H., Achouri, Y., Dubois, C., Bondue, A., Simons, B.D., Blanpain, C., 2014. Early lineage restriction in temporally distinct populations of Mesp1 progenitors during mammalian heart development. Nat. Cell Biol. 16, 829–840.

Lescroart, F., Hamou, W., Francou, A., Théveniau-Ruissy, M., Kelly, R.G., Buckingham, M., 2015. Clonal analysis reveals a common origin between nonsomite-derived neck muscles and heart myocardium. Proc. Natl. Acad. Sci. USA 112, 1446–1451.

Lescroart, F., Kelly, R.G., Le Garrec, J.-F., Nicolas, J.-F., Meilhac, S.M., Buckingham, M., 2010. Clonal analysis reveals common lineage relationships between head muscles and second heart field derivatives in the mouse embryo. Development 137, 3269–3279.

Lescroart, F., Mohun, T., Meilhac, S.M., Bennett, M., Buckingham, M., 2012. Lineage tree for the venous pole of the heart: clonal analysis clarifies controversial genealogy based on genetic tracing. Circ. Res. 111, 1313–1322.

Liao, J., Aggarwal, V.S., Nowotschin, S., Bondarev, A., Lipner, S., Morrow, B.E., 2008. Identification of downstream genetic pathways of Tbx1 in the second heart field. Dev. Biol. 316, 524–537.

Lin, L., Cui, L., Zhou, W., Dufort, D., Zhang, X., Cai, C.-L., Bu, L., Yang, L., Martin, J., Kemler, R., Rosenfeld, M.G., Chen, J., Evans, S.M., 2007. β-Catenin directly regulates Islet1 expression in cardiovascular progenitors and is required for multiple aspects of cardiogenesis. Proc. Natl. Acad. Sci. USA 104, 9313–9318.

Mandal, A., Holowiecki, A., Song, Y.C., Waxman, J.S., 2017. Wnt signaling balances specification of the cardiac and pharyngeal muscle fields. Mech. Dev. 143, 32–41.

Marvin, M.J., Di Rocco, G., Gardiner, A., Bush, S.M., Lassar, A.B., 2001. Inhibition of Wnt activity induces heart formation from posterior mesoderm. Genes Dev. 15, 316–327.

Meilhac, S.M., Esner, M., Kelly, R.G., Nicolas, J.-F., Buckingham, M.E., 2004. The clonal origin of myocardial cells in different regions of the embryonic mouse heart. Dev. Cell 6, 685–698.

Molenaar, M., van de Wetering, M., Oosterwegel, M., Peterson-Maduro, J., Godsave, S., Korinek, V., Roose, J., Destrée, O., Clevers, H., 1996. XTcf-3 transcription factor mediates beta-catenin-induced axis formation in Xenopus embryos. Cell 86, 391–399.

Naito, A.T., Shiojima, I., Akazawa, H., Hidaka, K., Morisaki, T., Kikuchi, A., Komuro, I., 2006. Developmental stage-specific biphasic roles of Wnt/beta-catenin signaling in cardiomyogenesis and hematopoiesis. Proc. Natl. Acad. Sci. USA 103, 19812–19817.

Nathan, E., Monovich, A., Tirosh-Finkel, L., Harrelson, Z., Rousso, T., Rinon, A., Harel, I., Evans, S.M., Tzahor, E., 2008. The contribution of Islet1-expressing splanchnic mesoderm cells to distinct branchiomeric muscles reveals significant heterogeneity in head muscle development. Development 135, 647–657.

Niida, A., Hiroko, T., Kasai, M., Furukawa, Y., Nakamura, Y., Suzuki, Y., Sugano, S., Akiyama, T., 2004. DKK1, a negative regulator of Wnt signaling, is a target of the β-catenin/TCF pathway. Oncogene 23, 8520–8526.

Olson, E.N., 2006. Gene regulatory networks in the evolution and development of the heart. Science 313, 1922–1927.

Park, M., Venkatesh, T.V., Bodmer, R., 1998. Dual role for the zeste-white3/shaggy-encoded kinase in mesoderm and heart development of Drosophila. Dev. Genet. 22, 201–211.

Park, M., Wu, X., Golden, K., Axelrod, J.D., Bodmer, R., 1996. The wingless signaling pathway is directly involved in Drosophila heart development. Dev. Biol. 177, 104–116.

Pickett, C.J., Zeller, R.W., 2018. Efficient genome editing using CRISPR-Cas-mediated homology directed repair in the ascidian Ciona robusta. Genesis, e23260.

Prall, O.W.J., Menon, M.K., Solloway, M.J., Watanabe, Y., Zaffran, S., Bajolle, F., Biben, C., McBride, J.J., Robertson, B.R., Chaulet, H., Stennard, F.A., Wise, N., Schaft, D., Wolstein, O., Furtado, M.B., Shiratori, H., Chien, K.R., Hamada, H., Black, B.L., Saga, Y., Robertson, E.J., Buckingham, M.E., Harvey, R.P., 2007. An Nkx2-5/Bmp2/Smad1 negative feedback loop controls heart progenitor specification and proliferation. Cell 128, 947–959.

Putnam, N.H., Butts, T., Ferrier, D.E.K., Furlong, R.F., Hellsten, U., Kawashima, T., Robinson-Rechavi, M., Shoguchi, E., Terry, A., Yu, J.-K., Benito-Gutiérrez, E., Dubchak, I., Garcia-Fernàndez, J., Gibson-Brown, J.J., Grigoriev, I.V., Horton, A.C., de Jong, P.J., Jurka, J., Kapitonov, V.V., Kohara, Y., Kuroki, Y., Lindquist, E., Lucas, S., Osoegawa, K., Pennacchio, L.A., Salamov, A.A., Satou, Y., Sauka-Spengler, T., Schmutz, J., Shin-I, T., Toyoda, A., Bronner-Fraser, M., Fujiyama, A., Holland, L.Z., Holland, P.W.H., Satoh, N., Rokhsar, D.S., 2008. The amphioxus genome and the evolution of the chordate karyotype. Nature 453, 1064–1071.

Razy-Krajka, F., Gravez, B., Kaplan, N., Racioppi, C., Wang, W., Christiaen, L., 2018. An FGF-driven feed-forward circuit patterns the cardiopharyngeal mesoderm in space and time. Elife, 7. http://dx.doi.org/10.7554/eLife.29656.

Razy-Krajka, F., Lam, K., Wang, W., Stolfi, A., Joly, M., Bonneau, R., Christiaen, L., 2014. Collier/OLF/EBF-dependent transcriptional dynamics control pharyngeal muscle specification from primed cardiopharyngeal progenitors. Dev. Cell 29, 263–276.

Saga, Y., Miyagawa-Tomita, S., Takagi, A., Kitajima, S., Miyazaki, J. i., Inoue, T., 1999. MesP1 is expressed in the heart precursor cells and required for the formation of a single heart tube. Development 126, 3437–3447.

Satoh, N., 1994. Developmental Biology of Ascidians. Cambridge University Press, New York, NY.

Satou, Y., Imai, K.S., Satoh, N., 2004. The ascidian Mesp gene specifies heart precursor cells. Development 131, 2533–2541.

Schmeckpeper, J., Verma, A., Yin, L., Beigi, F., Zhang, L., Payne, A., Zhang, Z., Pratt, R.E., Dzau, V.J., Mirotsou, M., 2015. Inhibition of Wnt6 by Sfrp2 regulates adult cardiac progenitor cell differentiation by differential modulation of Wnt pathways. J. Mol. Cell. Cardiol. 85, 215–225.

Schneider, V.A., Mercola, M., 2001. Wnt antagonism initiates cardiogenesis in Xenopus laevis. Genes Dev. 15, 304–315.

Shi, W., Hendrix, D., Levine, M., Haley, B., 2009. A distinct class of small RNAs arises from pre-miRNA-proximal regions in a simple chordate. Nat. Struct. Mol. Biol. 16, 183–189.

Squarzoni, P., Parveen, F., Zanetti, L., Ristoratore, F., Spagnuolo, A., 2011. FGF/MAPK/Ets signaling renders pigment cell precursors competent to respond to Wnt signal by directly controlling Ci-Tcf transcription. Development 138, 1421–1432.

Stolfi, A., Gainous, T.B., Young, J.J., Mori, A., Levine, M., Christiaen, L., 2010. Early chordate origins of the vertebrate second heart field. Science 329, 565–568.

Stolfi, A., Gandhi, S., Salek, F., Christiaen, L., 2014. Tissue-specific genome editing in Ciona embryos by CRISPR/Cas9. Development 141, 4115–4120.

Stolfi, A., Sasakura, Y., Chalopin, D., Satou, Y., Christiaen, L., Dantec, C., Endo, T., Naville, M., Nishida, H., Swalla, B.J., Volff, J.-N., Voskoboynik, A., Dauga, D., Lemaire, P., 2015. Guidelines for the nomenclature of genetic elements in tunicate genomes. Genesis 53, 1–14.

Takemaru, K.-I., Yamaguchi, S., Lee, Y.S., Zhang, Y., Carthew, R.W., Moon, R.T., 2003. Chibby, a nuclear beta-catenin-associated antagonist of the Wnt/Wingless pathway. Nature 422, 905–909.

Tirosh-Finkel, L., Elhanany, H., Rinon, A., Tzahor, E., 2006. Mesoderm progenitor cells of common origin contribute to the head musculature and the cardiac outflow tract. Development 133, 1943–1953.

Tzahor, E., 2007. Wnt/beta-catenin signaling and cardiogenesis: timing does matter. Dev. Cell 13, 10–13.

Tzahor, E., Evans, S.M., 2011. Pharyngeal mesoderm development during embryogenesis: implications for both heart and head myogenesis. Cardiovasc. Res. 91, 196–202.

Tzahor, E., Kempf, H., Mootoosamy, R.C., Poon, A.C., Abzhanov, A., Tabin, C.J., Dietrich, S., Lassar, A.B., 2003. Antagonists of Wnt and BMP signaling promote the formation of vertebrate head muscle. Genes Dev. 17, 3087–3099.

Tzahor, E., Lassar, A.B., 2001. Wnt signals from the neural tube block ectopic cardiogenesis. Genes Dev. 15, 255–260.

Ueno, S., Weidinger, G., Osugi, T., Kohn, A.D., Golob, J.L., Pabon, L., Reinecke, H., Moon, R.T., Murry, C.E., 2007. Biphasic role for Wnt/beta-catenin signaling in cardiac specification in zebrafish and embryonic stem cells. Proc. Natl. Acad. Sci. USA 104, 9685–9690.

Wang, W., Niu, X., Jullian, E., Kelly, R.G., Satija, R., Christiaen, L., 2017. A single cell transcriptional roadmap for cardiopharyngeal fate diversification. bioRxiv. ⟨https://doi.org/10.1101/150235⟩.

Wang, W., Racioppi, C., Gravez, B., Christiaen, L., 2018. Purification of fluorescent labeled cells from dissociated ciona embryos. Adv. Exp. Med. Biol., 101–107.

Wang, W., Razy-Krajka, F., Siu, E., Ketcham, A., Christiaen, L., 2013. NK4 antagonizes Tbx1/10 to promote cardiac versus pharyngeal muscle fate in the ascidian second heart field. PLoS Biol. 11, e1001725.

Wu, X., Golden, K., Bodmer, R., 1995. Heart development in Drosophila requires the segment polarity gene wingless. Dev. Biol. 169, 619–628.

Yamada, L., Kobayashi, K., Degnan, B., Satoh, N., Satou, Y., 2003. A genomewide survey of developmentally relevant genes in Ciona intestinalis. IV. Genes for HMG transcriptional regulators, bZip and GATA/Gli/Zic/Snail. Dev. Genes Evol. 213, 245–253.

Zhang, X., Abreu, J.G., Yokota, C., MacDonald, B.T., Singh, S., Coburn, K.L.A., Cheong, S.-M., Zhang, M.M., Ye, Q.-Z., Hang, H.C., Steen, H., He, X., 2012. Tiki1 is required for head formation via Wnt cleavage-oxidation and inactivation. Cell 149, 1565–1577.

Zhu, W., Shiojima, I., Ito, Y., Li, Z., Ikeda, H., Yoshida, M., Naito, A.T., Nishi, J.-I., Ueno, H., Umezawa, A., Minamino, T., Nagai, T., Kikuchi, A., Asashima, M., Komuro, I., 2008. IGFBP-4 is an inhibitor of canonical Wnt signalling required for cardiogenesis. Nature 454, 345.